LIQUID METAL INSIDE A HORIZONTALLY ROTATING CYLINDER UNDER VIBRATIONS

Jan BOHÁČEK•, Abdellah KHARICHA•, Andreas LUDWIG•, Menghuai WU•

Abstract: *During the horizontal spin casting of rolls, vibrations and mould deformations seems to have a significant effect on the final quality of the product. There are several sources for vibrations that can be found. Firstly, it is a poor roundness and a static imbalance of the chill itself. Secondly, those are free vibrations linked with natural frequencies. Due to the pouring of a liquid metal, solidification, and consequent shrinkage, the vibration characteristic is also evolving in time. In this paper we introduce sine-like vibrations in all directions except of axial. Next, we also consider a bending of the mould axis. Although this approach is rather intuitive and is not based on any experimental data, it is believed that it stands for a useful mathematical simplification of a real process. Both, vibrations and axis bending, are used as an input for CFD simulations of the flow dynamics of the liquid metal inside the rotating cylinder. The aim is to study the feedback of the free surface behavior in terms of wave propagation and various wave shapes, even though the solidification has not been implemented in the model yet. Shallow water equations were modified in order to simulate the flow of liquid inside the rotating cylinder. Besides forces resulting from vibrations, the following forces were applied: the centrifugal force, the friction force, the Coriolis force, and the gravity force. Effects of surface tension and wind friction were neglected.*

1. INTRODUCTION

The horizontal spin casting process (HSC) is a casting process that has generally several advantages above a traditional gravity casting process and also some other casting processes. The main profit is usually superior mechanical properties. Centrifugally cast

---

• Dr. Jan Bohacek, Materials Center Leoben Forschung GmbH, A–8700 Leoben, Roseggerstrasse 12, jan.bohacek@mcl.at

• Dr. Abdellah Kharicha, Chair of Simulation and Modelling of Metalurgical Processes, Department of Metallurgy, Montan University of Leoben, 8700 Leoben, Franz-Josef-Str. 18/III, abdellah.kharicha@unileoben.ac.at

• Prof. Andreas Ludwig, Chair of Simulation and Modelling of Metalurgical Processes, Department of Metallurgy, Montan University of Leoben, 8700 Leoben, Franz-Josef-Str. 18/III, andreas.ludwig@unileoben.ac.at

• Dr. Menghuai Wu, Chair of Simulation and Modelling of Metalurgical Processes, Department of Metallurgy, Montan University of Leoben, 8700 Leoben, Franz-Josef-Str. 18/III, menghuai.wu@unileoben.ac.at

products have a high degree of metallurgical purity and homogeneous microstructure. A significant gain is observed for the rupture strength, the rupture strain, the Young modulus. These properties naturally depend on the centrifugal force and thus, the higher the distance from the rotation center, the bigger the increase in mechanical properties. Of course, since the centrifugal force is defined as the product of the radius and the square of the angular frequency, the final mechanical properties mostly depend on the selection of the angular frequency. The proper selection of the angular frequency has to be done in order to prevent so-called raining on one hand i.e. metal droplets can fall down from the upper part of the inside surface of the casting product due to the low centrifugal acceleration and the winning counteracting of the gravity. On the other hand, excessive speeds can, however, lead to the longitudinal cracks caused by the hoop stress in the initially solidified layer. To make matters worse, it is not just the angular frequency that has to be properly chosen. The list of other important parameters could be as follows: the pouring temperature, the pouring rate, the mould coating etc. Apparently, the list of parameters should further be extended to account also for vibrations, no matter whether those are natural, forced or their combination. The reason for that might be found for example in [5], [6]. According to these studies, the centrifugal effect can be divided into three separate features: the centrifugal force, the intrinsic vibration, and the fluid dynamics. As regards the vibration effect, there was observed a transition from the lamellar to the fibrous morphology with the increase of the vibration amplitude. Vibrations were also proved to increase the eutectic volume fraction. However, a critical value of acceleration was found at which the grains tend to coarsen. They also reported some drop in the volume fraction and the size of pores, but again a critical value of acceleration most likely exists. It is well-known that during the centrifugal casting the melt firstly solidifies on the mould wall, but due to the turbulent flow germens are being pulled out back into to the melt and stand as a new nucleation points [7]. It is believed that vibrations can significantly enhance this process.

So far the most important aspects of the centrifugal casting were outlined and even a non-expert has to admit that due to the complexity of the problem it is useful to divide the solution of the problem into a step-by-step process.

The present paper is focused solely on a numerical modelling of the cold flow of the liquid film. (The solidification process will be included later.) The main objective was to study different wave patterns formed on the free surface of the liquid film caused by acting of inertial and body forces. From the observation (see Figure 1) of the real casting process the melt was evidently rotating with the mould and hence, the fluid flow was modelled in the rotating frame of reference i.e. fictitious forces (the centrifugal force, the Coriolis force) were implemented.

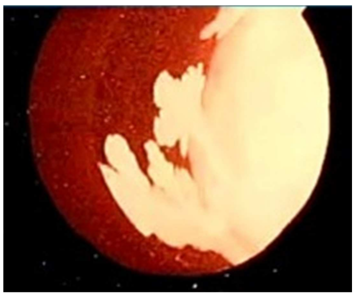

Figure 1 Snapshot of the spreading liquid metal inside the rotating mould

It should be yet briefly mentioned endeavours of other researches who also dealt with this problem numerically. An attempt for a comprehensive description of the flow dynamics of the melt inside the horizontally rotating mould can be found in [8]. The VOF model was set up in STAR-CD. Two phases were simulated, the liquid metal and the surrounding air, with the filling system included. The time step was notably high (~0.01 s) which implies a very rough mesh. Interestingly, the results were in a very good agreement with experimental data. In [9] the research was contrarily concentrated on a complete description of centrifugal casting of aluminium melt containing ceramic particles. The model took into account propagation of the solid liquid interface and also movement of ceramic particles due to centrifugal force, but was designed only as one dimensional. In spite of model complexity, it did not give any information about the fluid flow. Benilov ([10], [11]) studied instabilities of a liquid film inside a horizontally rotating cylinder using the leading-order lubrication approximation. Viscosity and gravity were assumed dominant, whereas hydrostatic pressure and inertia were treated as perturbations. Asymptotic equations were defined as an eigenvalue problem and imaginary part of the complex frequency was calculated for different dimensionless parameters to test the stability of the liquid film. It was concluded that inertia always causes instability, whereas hydrostatic pressure does not affect the stability at all. As regards surface tension, a two-fold effect on eigenmodes was detected. On one hand, the contribution of surface tension to the grow rate is always negative; thus, it is stabilizing. On the other hand, it was shown that unstable solutions can arise from the interaction between the surface tension and (anti)diffusion terms. Mahadevan [12] solved numerically 3D N-S equations expressed in dimensionless form in cylindrical coordinates. Keeping in mind the very small ratio between the characteristic length scale of the liquid film and the cylinder radius, he eliminated the radial velocity by integrating the continuity equation over the height of the film. His model was successful in capturing recirculating regions and also so-called shark-teeth pattern [13].

2. Numerical Model

It is based on so-called shallow water equations, in some publications referred to as a geostrophic model. In layman's terms, one could take it as a 2.5D model. The fundamental model theory can be found e.g. in [1]–[3]. Here, the model was applied using the most general multiphase model available in the commercial CFD package FLUENT (Euler-Euler model).

In general, the shallow water equations are used for modelling purposes of oceanography and also belong to basic modelling tools of meteorologists. For this reason, the shallow water equations are usually defined in rotating spherical geometry. Generally, two main simplifications are introduced and are known as the traditional and the hydrostatic approximation. The first one neglects so-called metric terms coming out from the spherical geometry. The second one neglects all vertical components in momentum equations except of pressure gradient and buoyancy force. Very often due to large lengthscales involved it is common to assume inviscid flow. Next, the velocity along the liquid height is constant. A multiple layer approach is usually used to simulate vertical liquid mixing that might be for example caused by a density difference.

The main differences of the current numerical model used in this study against the shallow water model summarized above are as follows. Our model is based on one layer approach. (Later on, it will be extended to the two layer approach in order to simulate the whole solidification process. Next, it will further expand to the third layer, which will represent the mushy zone.) In the text below our model is simply referred to as the model. Since the liquid has a notably high viscosity and from observations it more or less rotates with the mould, the laminar flow is expected and hence, the parabolic velocity profile is included. On the cylindrical wall no slip BC condition is considered. The model is designated for cylindrical coordinates. For Fluent code it, however, had to be transformed into Cartesian coordinates. The continuity equation has a fairly familiar definition:

$$\frac{\partial h}{\partial t} + \nabla \cdot \left(h\vec{u} \right) = 0, \tag{1}$$

where h denotes the height of the liquid film. The momentum equations in differential form for x and y coordinates are defined by the following equation

$$\frac{D}{Dt}\left(h\rho\vec{u} \right) = -h\nabla p + h\mu\nabla^2\vec{u} + \rho\vec{g} - \rho h\Omega^2 (R-h)\nabla h - 2\rho h\vec{\Omega}\times\vec{u} - 2\mu\frac{\vec{u}}{h}, \tag{2}$$

The term on the left-hand side of (2) is the well-known material derivative of the velocity vector field but multiplied by the liquid height. On the RHS of (2) several different terms should be explained. The first term is the force induced due to the gradient of the static pressure. Next, the second term handles the momentum losses resulting from stress tensor but only in tangential and axial direction. The last four terms represent the gravity force, the centrifugal force, the Coriolis force and the friction force with the wall, respectively. More detailed information on derivation is available in [4] and will not be discussed here.

3. VIBRATIONS AND AXIAL BENDING OF CYLINDER

In order to account for vibrations the model had to be significantly modified. In the first place, the term of the axial bending and vibrations must be explained and defined in the vector form. The cylinder is rotating around its horizontal axis and is supported by four rollers. On one side the two coaxial rollers are driving, while on the other side the next two are just driven.

As regards the axial bending, it is assumed to have a sinusoidal shape with the two nodes positioned exactly in rollers. The slope of bending is given by the following formula:

$$\tan\theta = A\frac{\pi}{\lambda}\cdot\sin\left(\frac{\pi x}{\lambda}\right), \tag{3}$$

where A is the amplitude of bending, x is the axial coordinate, and λ is the distance between two coaxial rollers (Figure 2). In the rotating frame of reference this bending is time independent.

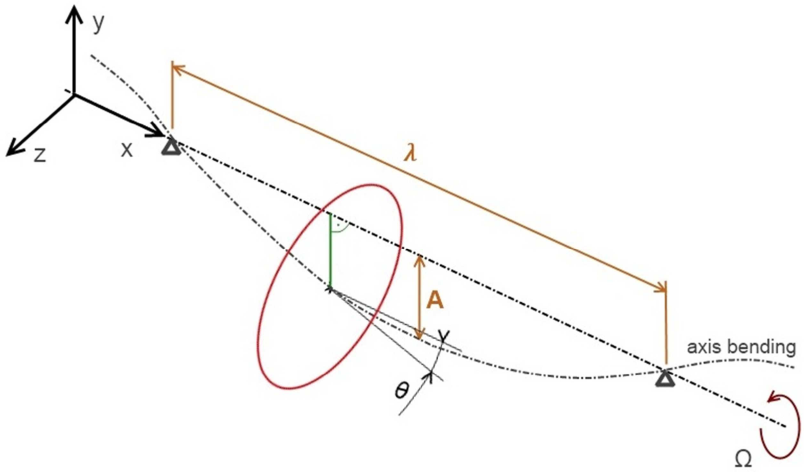

Figure 2 Sine-like axis bending

As briefly noted in abstract, vibrations can have several different origins that can consequently result in rather complicated mathematical description. In this paper vibrations are considered to be solely arising from the poor roundness of the cylinder and do not change along the axis of rotation. One could imagine them as a time–dependent perturbation of gravity. In vector form it can be defined as:

$$\overrightarrow{a_v}(0, \quad \xi\cos(\omega t+\beta), \quad \xi\sin(\omega t+\beta)), \tag{4}$$

where ξ is the amplitude of acceleration due to vibrations, ω is the angular frequency associated to vibrations, and finally β is the phase. The phase β specifies where the oscillation begins. In the model it was kept constant equal to $\pi/2$. The angular frequency ω was set to the double of the angular frequency Ω of the rotating cylinder. This was only based on assuming the elliptical cross section of the cylinder that naturally results in the double. From (4) it is evident that the acceleration a_v is always zero in axial direction. Unlike the implementation of vibrations into the model, the bending of axis has an effect on all the forces listed in brackets (the gravity, the centrifugal force, the Coriolis force, and even the force due to vibrations itself). Before giving a mathematical background for modification of all these four forces, two different Cartesian coordinate systems must be defined. The first one denoted as $C_1(\vec{x},\vec{y},\vec{z})$ is a global coordinate system, where x-axis is going through the nodes mentioned above and y- and z-axis are rotating with angular frequency Ω. The second one denoted as $C_2(\vec{c},\vec{d},\vec{r})$ is a local coordinate system, where $\vec{c}$ is a unit vector parallel to the cylinder axis identical to the bending line. The unit vector $\vec{d}$ is aligned with the tangent to the cylindrical surface oriented in positive direction. At last, the unit vector $\vec{r}$ is perpendicular to the cylindrical surface and oriented outwards. Note, the coordinate system C_2 is consistent with, say, the coordinate system C_3 used in FLUENT code and one can write:

$$C_2(\vec{c},\vec{d},\vec{r}) = C_3(\vec{x}',\vec{y}',0), \tag{5}$$

where 0 signifies that the problem is solved only in 2 dimensions. The gravity acceleration was transformed into C_2 using the following formulas:

$$g_c = \vec{g} \cdot \vec{c}, \quad g_d = \vec{g} \cdot \vec{d}, \quad g_r = \vec{g} \cdot \vec{r}, \tag{6}$$

The centrifugal, the Coriolis accelerations, and the acceleration due to vibrations were transformed analogically. Non-zero components in the $\vec{r}$ direction were multiplied by the liquid density, integrated over the liquid height and expressed as a hydrostatic pressure p_h. The source terms for both the $\vec{c}$ and the $\vec{d}$ direction resulting from the pressure p_h are given by:

$$S_{x'} = \int_0^h \frac{\partial p_h}{\partial x'} dr, \quad S_{y'} = \int_0^h \frac{\partial p_h}{\partial y'} dr \tag{7}$$

4. NUMERICAL RESULTS

All simulations were run with constant physical properties of the liquid metal (ρ=6800 kg/m^3, μ=0.006 kg/m-s). Concerning the geometry, the cylinder radius was 0.372 m with the length of 3.2 m. Two different angular frequencies Ω were considered (30 rad/s and 71.2 rad/s), from which the first one was just arbitrarily chosen and the second one on the contrary represents the value used in the real casting process. Several heights h_{avg} of the liquid were calculated (5, 10, 20, 30, 40 mm), where the subscript *avg* implies an average height of the liquid layer. Note that the filling of the liquid was not included in the model, but the initial distribution of the liquid height was rather imposed. Two distinct initial distributions were considered. It was either a distribution with a constant liquid height h_0 equal h_{avg} or it was perturbed using the following function:

$$h_0 = h_{avg}\left[\sin\left(a\cdot(x'-b)^2\right)+\sin\left(c\cdot(y'-d)^2\right)\right], \tag{8}$$

where constants a, b, c, and d were 10, 0.4, 12, and 0.3, respectively. This function (8) was chosen in order to perturb the free surface with different wavelengths in both directions (x′ and y′).

Several cases labeled from N1 to N10 were calculated with the model settings listed in Table 1. The time step was held constant (Δt=0.001 s) and the local Courant number was always less than 0.1. The time discretization was second-order implicit. Firstly, results were compared in terms of mean amplitude, which was defined as a difference between the minimum and the maximum liquid height found in the entire computational domain divided by two. In Figure 3, plots of the mean amplitude are shown for the angular frequency of 71.2 rad/s. Note the grey data in Figure 3, which represent the data from simulation. For post-processing purposes each data set was rather convolved with the Gaussian kernel to make a picture more clear. Results for Ω=30 rad/s are presented in Figure 4. Several general features can be found:

1) Mean amplitudes never drop to zero within the calculated time range (≈180 s). Certain waves survive even for small h_{avg}.
2) A single longitudinal wave is formed in early stages due to the gravity and the inertia interaction no matter whether the free surface was initially perturbed or not. As the velocity field develops, the longitudinal wave diminishes within the apparent relaxation time ranging from 20 s to 40 s.
3) The higher the h_{avg}, the higher the mean amplitude.

Table 1 List of model settings for cases N1–N10

	Ω [rad/s]	h_{avg} [mm]	vibrations [-]	initial perturbation [-]
N1	71.2	5	ON	ON
N2		10		
N3		20		
N4		30		
N5		40		
N6		5		OFF
N7		10		
N8	30	20		
N9				ON
N10			OFF	OFF

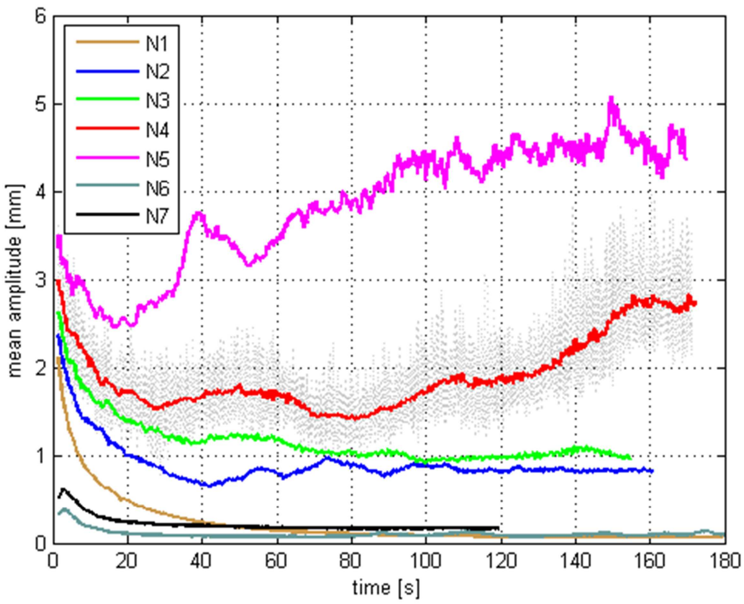

Figure 3 Time-dependent mean amplitude for Ω=71.2 rad/s

N1 (initial perturbation) and N6 (h_0=constant) converge to the same value of mean amplitude. On the contrary, N2 (initial perturbation) and N7 (h_0=constant) do not.

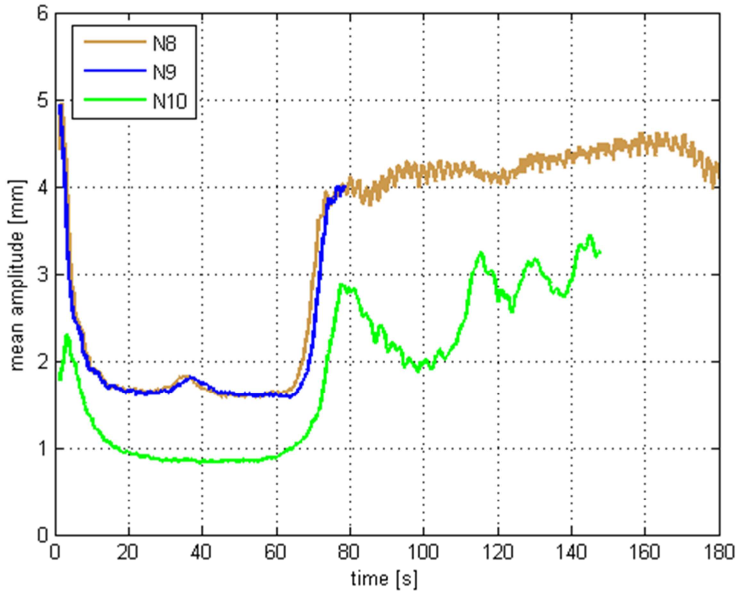

Figure 4 Time-dependent mean amplitude for Ω=30 rad/s

In Figure 4, the initial state of the free surface, however, has no effect on the mean amplitude (N8, N9). Note the relatively calm region from 20 s to 60 s with a sudden transition to instability at 60 s. N10 with no vibrations involved is significantly different compared to N8. Vibrations evidently amplify the mean amplitude in the whole time range. Further, the mean amplitudes of N10 significantly fluctuate in time.

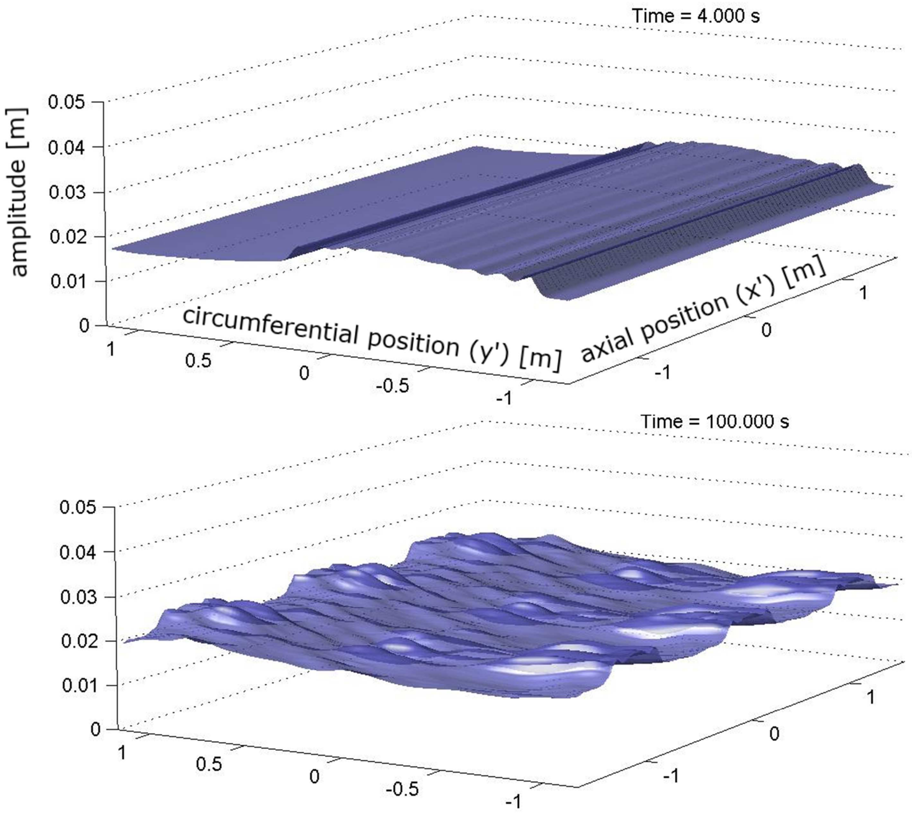

Figure 5 Actual shape of free surface for N8 at times 4 s and 100 s

In Figure 5, actual shapes of the free surface are shown in the plane x′y′. Note that the y′ coordinate stands for the circumferential position on the cylinder. The upper plot shows a single wave travelling along the cylinder circumference at 4 s, whereas the lower plot signifies a fully-developed wave pattern with rather annular waves at 100 s.

5. CONCLUSIONS AND FUTURE PROSPECTS

The model based on the shallow water equation was developed and successfully implemented in the commercial CFD package FLUENT. It is designated for simulation of liquid flows inside a horizontally rotating cylinder. The objective was to study wave patterns of the free surface, wave birth, propagation, and death. Besides, the aim was also to study a response of the system on different initial conditions i.e. the initial liquid height h_0 was either constant or perturbed using a sine-like function (see Equation (8)). The main assumptions of the model are: The angular frequency Ω of the cylinder (or the fluid viscosity μ) is so high that the fluid is mainly rotating with the cylinder. For this reason, the model could be defined in the rotating frame of reference. Next, the parabolic velocity profile along the liquid height is taken into account with no slip boundary condition on the cylindrical wall.

The model was further extended in order to account for vibrations and an axis bending. Both, the vibrations and the axis bending, were defined using trigonometric functions. This approach is supported by [14]. The model was set up using the Euler-Euler model and solved in the 2D double-precision solver with the second-order implicit time discretization.

Several cases were calculated with changing four parameters (h_{avg}=5, 10, 20, 30, or 40 mm; Ω = 30 or 71.2 rad/s; vibrations either ON or OFF; initial perturbations or h_0=constant). In all cases one longitudinal wave was formed in early stages no matter the initial conditions of the free surface, then it was gradually damped and finally either a noticeable transition to instability occurred or the mean amplitude just dropped to a roughly constant value (never zero). Next, it was shown that for smaller h_{avg} (5 mm) the initial condition of the free surface does not affect the mean amplitude in fully-developed regime. However, for higher h_{avg} (10 mm) the mean amplitudes of the fully-developed flow were totally different (higher for the case with the initial perturbations than for the case with a constant h_0). Generally, wave patterns of all the case with Ω=30 rad/s resembled the annular flow, whereas the cases with Ω=71.2 rad/s gave rather helicoid waves travelling from both ends of the cylinder.

To sum up, despite extremely high centrifugal forces (~100 G) acting on a liquid layer the interaction between the inertia, the gravity, and the vibrations can lead to the formation of waves on the free surface. The higher the liquid height is, the more it is prone to instabilities. This is practically driven by the wall friction term (see Equation (2)), which always stabilizes the liquid layer and is naturally more dominant for smaller liquid heights.

We still have yet to perform mesh sensitivity tests. It would be also useful to refine the ranges of parameters (Ω, h_{avg}) in order to have more detailed map of results. Further, we plan to collect data from the measurement of vibrations from the industrial partner with the recording frequency >100 Hz. These data will be transformed into the frequency spectrum, compared with our simplified model for vibrations, and finally the model could be possibly modified. Next, the solidification will be included using the second layer approach taking into account the heat conduction inside the mould and also heat losses into ambient. Finally, the mushy zone might be possibly accounted for using the third layer considering a more complex velocity profile along its height.

6. ACKNOWLEDGEMENT

This work is financially supported by the Material Center Leoben and the Eisenwerk Sulzau–Werfen.

REFERENCES

[1] Faber, T.E.: Fluid Dynamics for Physicist, Cambridge University Press, 1995, 440 pp.
[2] Kundu, P.K.: Fluid Mechanics, Academic Press, 1990, 648 pp.
[3] Dellar, P.J.: Shallow water equations with a complete Coriolis force and topography, Physics of Fluids vol. 17, 2005, 2–23 pp.
[4] Bohacek, J., Kharicha, A., Ludwig, A., Wu, M.: Shallow water equations for a liquid film in horizontally rotating cylinder, Liberec, Experimental Fluid mechanics, pp., 2011
[5] Chirita, G., Stefanuscu, I., Barbosa, J., Puga, H., Soares, D., Silva, F. S.: On assessment of processing variables in vertical centrifugal casting technique, International Journal of Cast Metals Research, 2009, 382–389 pp.
[6] Chirita, G., Stefanuscu, I., Soares, D., Silva, F. S.: Centrifugal versus gravity casting techniques over mechanical properties, Anales de Mecánica de la Fractura, 2006, 317–322 pp.
[7] Chang, S.R., Kim, J.M., Hong, C. P.: ISIJ International, 2001, 738–747 pp.
[8] Keerthiprasad, K. S., Murali, M. S., Mukunda, P. G., Majumdar, S.: Numerical Simulation and Cold Modeling experiments on Centrifugal Casting, Metallurgical and Materials Transactions B, vol. 42, 2010, 144–155 pp.
[9] Raju, P. S. S., Mehrotra, S. P.: Mathematical Modelling of Centrifugal Casting of Metal Matrix Composites, Material Transactions, JIM, vol. 41,2000, 1626–1635 pp.
[10] Benilov, E. S., Kopteva, N., O'Brien, S. B. G.: Does surface tension stabilize liquid films inside a rotating horizontal cylinder?, Q. JI Mech. Appl. Math., vol. 58, 2004, 185–200 pp.
[11] Benilov, E. S., O'Brien, S. B. G.: Inertial instability of a liquid film inside a rotating horizontal cylinder, Physics of fluids, vol. 17, 2005
[12] Hosoi, A.E., Mahadevan, L.: Axial instability of a free-surface front in a partially filled horizontal rotating cylinder, Physics of Fluids, vol. 11, 1999, 97–106 pp.
[13] Thoroddsen, S. T., Mahadevan, L.: Experimental study of coating flows in a partially-filled horizontally rotating cylinder, Experiments in Fluids, vol. 23, 1997
[14] Martinez, G., Garnier, M., Durand, F.: Stirring phenomena in centrifugal casting of pipes, Applied Scientific Research, vol. 44, 1987, 225–239